

DTC-based Position and Velocity Control for PM LSM Carrier at Low Speed Range

Linni Jian, Liming Shi and Yaohua Li

Institute of Electrical Engineering, Chinese Academy of Science, Beijing, P. R. China

Tel: +86-010-62527658, Fax: +86-010-62553871

Email: limings@mail.iee.ac.cn

ABSTRACT: This paper presents propulsion control for a carrier driven by permanent magnet linear synchronous motor (PM LSM) at low speed range. Direct thrust control (DTC) is applied in the control scheme, which is derived from the direct torque control used in rotary motors. In the control system, two feedback loops are used in order to realize high precise position and velocity control. The experiment results demonstrate that direct thrust control is an effective method to realize good speed and position control for PM LSM carrier at low speed range.

1 INTRODUCTION

In the modern transit systems, linear motor propulsion technology has been paid increasing attention. Linear motor transit system, which is benefit for earth environment, makes possible super high-speed and mass transportation. It can also accommodate to steep slopes and sharp turns.

In order to research the propulsion control technology for linear motor, a set of linear synchronous motor carrier system has been built up in our Lab. It consists of two sets of long-stator (long armature windings) PM LSMs that are driven independently by two inverters. Permanent magnets are mounted at the bottom of the carrier. Fig.1 shows the external view of the system in our Lab.



Figure 1: External view of the carrier system

Direct thrust control (DTC) is applied in the control scheme, which is derived from the direct torque control used in rotary motors^[1]. In order to realize high precise position and velocity control, two feedback loops are used. In this paper, the construction of the carrier system is described first. Then, the fundamental of the DTC is analyzed. Finally, the experimental results are given, which demonstrate

that DTC is an effective method for PM LSM especially at low speed range.

2 SYSTEM CONFIGURATION

Fig. 2 shows the cross section of the carrier system. The guideway is about 6 m in length. The carrier which is about 65 kg in weight is supported by four rollers to move on the the guideway. The armature windings of PM LSMs are installed on the two sides of the guideway. Fig. 3 indicates the structure of the carrier with four permanent magnets that are mounted in each corner at bottom. Table 1 shows the specifications of the whole system.

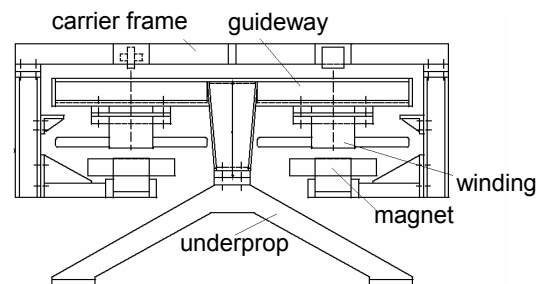


Figure 2: The cross section of the carrier system

The accurate electrical parameters of the PM LSM are needed in order to realize direct thrust control when carrier moves at low speed range. These parameters include stator resistance R_s , armature inductance L_d , L_q and permanent magnet flux linkage λ_{pm} .

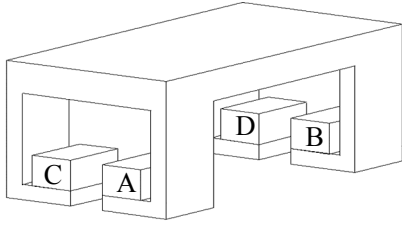


Figure 3: The structure of the carrier

Table 1: Specifications of the carrier system

Carrier	Size	200×600×700 mm
	Weight	65 kg
	Maximum load	60 kg
	Pole pitch	87 mm
PM LSM	Number of phase	3
	Number of poles	6
	Pole pitch	87 mm
	Rated current	13 A
	Gap length	5 mm
Guide Way	Width	0.5 mm
	Length	6 m
	Height	0.15 mm

Stator resistance is conveniently detected by 电桥仪器. Through analyzing the transition process of the stator current caused by injecting pulse DC voltage into armature windings, armature inductance L_d and L_q can be obtained. By keeping carrier still in different position on the guide way and injecting DC current into armature windings, the effective PM flux, which is coupled with stator windings, can be figured out by testing the electromagnetic force. Fig. 4 shows the static force test results which illustrate that the electromagnetic force is related with stator current (i_a) and the relative position (δ) between permanent magnet and armature axis, where, the relative position δ is represented in form of electrical load angle. Table 2 shows the electrical parameter detection results for PM LSM.

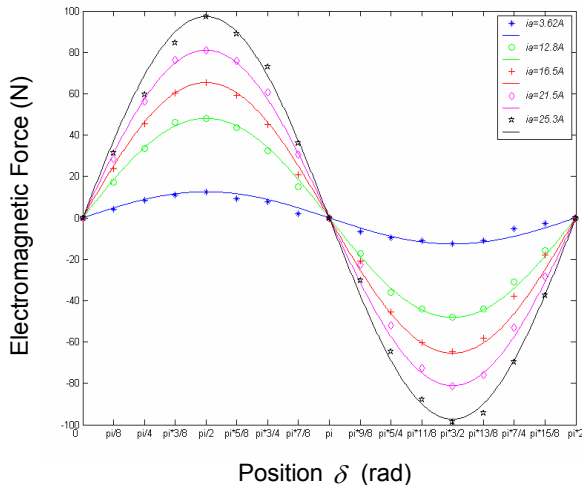


Figure 4: The test results of static force

Table 2: Specifications of the carrier system

Number of pole pairs n_p	3
Stator resistance R_s	0.84Ω
Stator d-axes inductance L_d	7 mH
Stator q-axes inductance L_q	8 mH
PM flux linkage λ_{pm}	1.2 mWb

3 DIRECT THRUST CONTROL FOR PM LSM

3.1 Math Equations of PM LSM

The PM LSM can be modeled in the mover reference frame (d-q) as follows:

$$\begin{bmatrix} v_{qs} \\ v_{ds} \end{bmatrix} = \begin{bmatrix} r_s & 0 \\ 0 & r_s \end{bmatrix} \cdot \begin{bmatrix} i_{qs} \\ i_{ds} \end{bmatrix} + \begin{bmatrix} p & \pi v/\tau \\ -\pi v/\tau & p \end{bmatrix} \cdot \begin{bmatrix} \lambda_{qs} \\ \lambda_{ds} \end{bmatrix} \quad (1)$$

$$\begin{bmatrix} \lambda_{qs} \\ \lambda_{ds} \end{bmatrix} = \begin{bmatrix} L_q & 0 \\ 0 & L_d \end{bmatrix} \cdot \begin{bmatrix} i_{qs} \\ i_{ds} \end{bmatrix} + \begin{bmatrix} 0 \\ \lambda_{pm} \end{bmatrix} \quad (2)$$

$$F = \frac{3}{2} \frac{\pi}{\tau} n_p [(L_d - L_q) i_{ds} i_{qs} + \lambda_{pm} i_{qs}] \quad (3)$$

where λ_{pm} , L_d , L_q are the permanent magnetic flux linkage, armature inductances, respectively. n_p is the pole pair number, p is the differential operate.

$$\lambda_{sd} = \lambda_s \cos \delta \quad \lambda_{sq} = \lambda_s \sin \delta \quad (4)$$

where λ_s represents the amplitude of the stator flux linkage.

Substituting (4) into (3), we obtain

$$F_x = \frac{3}{2} \frac{n_p \pi}{\tau \cdot L_d} \lambda_s \lambda_{pm} \sin \delta + \frac{3 \pi n_p (L_d - L_q)}{4 \tau \cdot L_d L_q} \lambda_s^2 \sin 2\delta \quad (5)$$

Equation (5) shows that the electromagnetic force is the function of load angle δ . By adjusting the stator voltage vector, it is convenient to change δ as well as F_x . This is the basic concept of DTC.

3.2 Fundamental of DTC for PM LSM

The scheme of conventional two-level voltage source inverter is shown in Fig.5. It can supply 8 different voltage vectors, in which, v_0, v_7 are zero vectors.

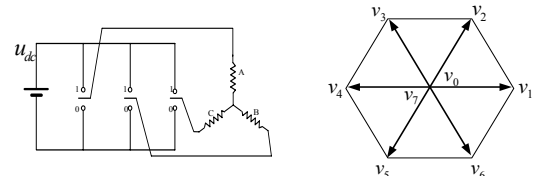


Figure 5: Two level voltage source inverter and the voltage vectors

$$V_s = \frac{2}{3} \cdot V_{dc} (S_a + S_b \cdot e^{j\frac{2}{3}\pi} + S_c \cdot e^{j\frac{4}{3}\pi}) \quad (6)$$

$$|v_i| = V_{dc} \quad (i=1\sim 6) \quad (7)$$

Where V_{dc} is the inverter DC voltage, S_a , S_b , S_c represent the switch situation of the phase a, b and c respectively. If the upper switch is on, it equals "1"; otherwise, it equals "0".

The stator flux linkage λ_s is controlled by applying these voltage vectors. During the switching interval (Δt), each voltage vector is constant, and the voltage equation (1) can be rewritten as follow:

$$\lambda_s(t + \Delta t) = v_s \Delta t - r_s \int i_s dt + \lambda_s(t) \quad (8)$$

Neglecting the small voltage drop on stator resistance, equation (8) implies that the end of the stator flux vector λ_s will move in the direction of the applied voltage vector. Supposing that during each sampling period the carrier stays still, the load angle δ is changed, and F_x is changed as well by adjusting the stator voltage vector.

The vector plane is divided into six zones, as shown in Fig. 6. In each zone, two adjacent voltage vectors are selected to increase or decrease the amplitude of λ_s , and also increase or decrease the load angle δ , respectively. Through choosing proper voltage vector in each zone, the end of λ_s will move in a ring.

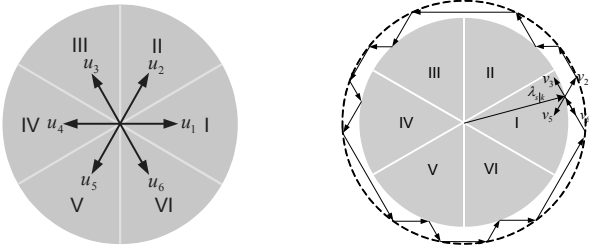


Figure 6: Plane division and the control of stator flux linkage

Force hysteresis controller and flux hysteresis controller are used to obtain quick output response. The switching functions are given as follows:

$$\Delta \lambda_s = \begin{cases} 1 & \lambda_s^* - \hat{\lambda}_s > \xi_1 \\ 0 & \lambda_s^* - \hat{\lambda}_s < -\xi_1 \end{cases} \quad (9)$$

$$\Delta F_x = \begin{cases} 1 & F_x^* - \hat{F}_x > \xi_2 \\ 0 & F_x^* - \hat{F}_x < -\xi_2 \end{cases} \quad (10)$$

where, λ_s^* , F_x^* are stator flux linkage reference and electromagnetic force reference respectively. $\hat{\lambda}_s$, \hat{F}_x are estimation results of λ_s and F_x respectively. ξ_1 , ξ_2 are the tolerances of the hysteresis controllers.

Fig. 7 illustrates the system structure of the direct thrust control for one PM LSM. In the stator reference frame, the stator flux linkage and the electromagnetic torque are estimated from the measured values of voltage and current by the following equations:

$$\lambda_{s\alpha} = \int_0^t (v_{s\alpha} - i_{s\alpha} r_s) dt + \lambda_{s\alpha 0} \quad (11)$$

$$\lambda_{s\beta} = \int_0^t (v_{s\beta} - i_{s\beta} r_s) dt + \lambda_{s\beta 0} \quad (12)$$

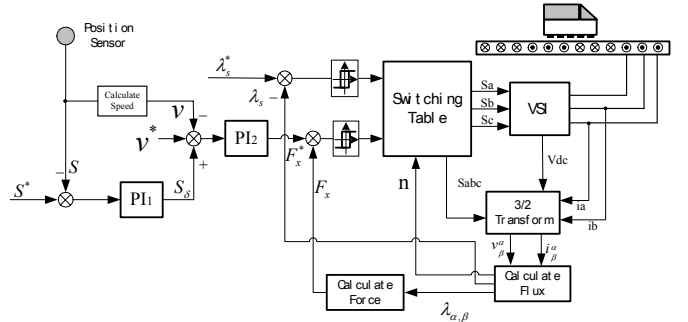
$$\lambda_s = \sqrt{\lambda_{s\alpha}^2 + \lambda_{s\beta}^2} \quad (13)$$

$$\theta_s = \arctan \frac{\lambda_{s\beta}}{\lambda_{s\alpha}} \quad (14)$$

$$F_x = \frac{3 n_p \pi}{2 \tau} (\lambda_{s\alpha} i_{s\beta} - \lambda_{s\beta} i_{s\alpha}) \quad (15)$$

However, during the low speed range, the armature back electromotive force is rather small. The stator flux linkage can not be precisely estimated by equation (11~14), so the current mode is adopted in this case:

$$\lambda_{sd} = L_d \cdot i_{sd} + \lambda_{pm} \quad (16)$$



$$\lambda_{sq} = L_q \cdot i_{sq} \quad (17)$$

Figure 7: The scheme of DTC system for PM LSM

The electromagnetic force reference is determined by route PI adjuster and speed PI adjuster. The control regulations are given as

$$S_\delta = K_{p1}(S^* - S) + K_{I1} \int (S^* - S) dt \quad (18)$$

$$F_x^* = K_{p2}(v^* - v + S_\delta) + K_{I2} \int (v^* - v + S_\delta) dt \quad (19)$$

4 EXPERIMENTAL RESULTS

Control algorithms were realized by DSP TMSLF 2407 based digital control system. The sampling period is set as 0.1 ms. Two sets of photoelectric en-

coder system are used to detect the instantaneous position of the carrier. During every double pole pitch range (360° electrical angle), there are 29 voltage pulses fed back to processor. The parameters of the PI adjustors are shown in Table 3.

Table 3: Parameters of the PI adjustors

	K_p	K_I
Route Adjuster	100	80
Speed Adjuster	40	5

Fig. 8 shows the armature current (phase A) waveform, when the carrier moves at some constant speed: In case A, the reference speed is set as 0.05m/s. Since the armature pole pitch is 0.087m, the synchronous frequency can be calculated as 0.287Hz. In case B, the reference speed is set as 0.1m/s, and the synchronous frequency is 0.575Hz. Fig. 9 depicts the armature current (phase A) waveform, when the carrier moves at some varying speed: In case A, the reference speed changes abruptly from 0.1m/s to -0.1m/s. In case B, the reference speed changes from 0.1m/s to 0.2m/s.

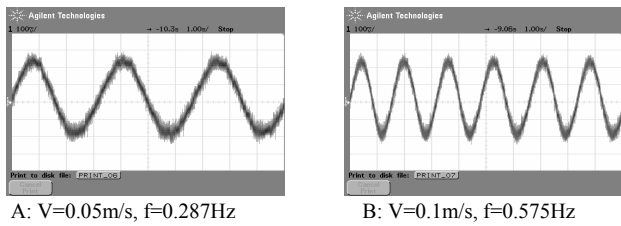


Figure 8: The armature current waveform (phase A) when reference speed is constant.

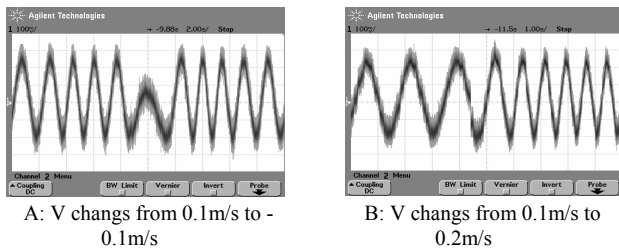


Figure 9: The armature current waveform (phase A) when reference speed is varying.

Design a reference speed curve for the carrier system, as shown in (19). It contains 6 phases: speed-up, steady move, speed-down, reverse speed-up, reversely steady move and reverse speed-down. The maximum single-track distance is 5m, and the maximum speed is 0.5m/s.

Fig.10 shows the experimental results. Fig. 10(a) gives the reference speed (up) and real speed (down). Fig. 10 (b) gives the reference position (up) and real position (down). Fig. 10(c) gives the armature current waveform. In the speed-up and speed-down phases, the peak value of the current is 7A, In the steady move phase, the peak value is 3A. Fig.

10(d) gives the electromagnetic force curve. The maximum value is 20N.

$$v = \begin{cases} 0.25t & 0 < t < 2(s) \\ 0.5 & 2 < t < 10(s) \\ 0.5 - 0.25t & 10 < t < 14(s) \\ -0.5 & 14 < t < 22(s) \\ 0.25t - 0.5 & 22 < t < 24(s) \end{cases} \quad (20)$$

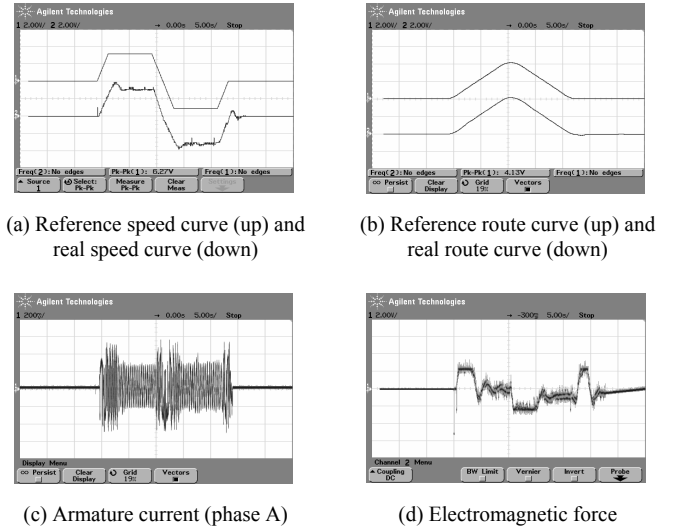


Figure 10: Experiment results when the carrier moves according to designed speed curve

5 CONCLUSIONS

The direct thrust control has been successfully applied in a set of linear motor carrier which is impelled by two sets of long-stator PM LSM. The experiment results demonstrate that direct thrust control is an effective method to realize good speed and position control for PM LSM carrier at low speed range.

REFERENCE

- 1.Zhong, L. & Rahman, M. F. 1997. Analysis of direct torque control in permanent magnet synchronous motor drive, *IEEE transactions on power electronics*. Vol. 12, No.3 528-535.1997.
- 2.Yoshida, K. & Takami, H. 2004. Smooth section crossing of controlled-repulsive PM LSM vehicle by DTC method based on new concept of fictitious section, *IEEE transaction on industrial electronics*. Vol. 51, No. 4 821-826. 2004.
- 3.Takahashi, I. 1993. Decoupling control of thrust and attractive force of a LIM using a space vector control inverter. *IEEE transactions on industry application*. Vol. 29, No. 1 161-167. 1993.
- 4.Jian, L. & Shi, L. 2005. Stability analysis for direct torque control of permanent magnet synchronous motors. *ICEMS 2005*. 1672-1675.